Multi-objective Bayesian global optimization for continuous problems and applications

Yang, K.

Author: Yang, Kaifeng
Title: Multi-objective Bayesian global optimization for continuous problems and applications
Date: 2017-12-06

Chapter 5

Preference-Based Multi-Objective Optimization

The ultimate goal of multi-objective optimization is to provide potential solutions to a decision maker. Usually, what concerns a decision maker concerns is a Pareto front in an interesting/preferred region, instead of the whole Pareto front. In this chapter, a method for effectively approximating a Pareto-front approximation set in the preferred region, based on multi-objective efficient global optimization (EGO), is introduced. EGO uses Gaussian processes (or Kriging) to build a model of the objective function. Our variant of EGO uses truncated expected hypervolume improvement (TEHVI) as an infill criterion, which takes into consideration predictive mean, variance and preference region in the objective space. Compared to expected hypervolume improvement (EHVI), the probability density function in TEHVI follows a truncated normal distribution. This chapter proposes a TEHVI method that makes it possible to set a region of interest on the Pareto front and focuses the search effectively on this preferred region. An expression for the exact and efficient computation of the TEHVI for truncation over a two dimensional range is derived, and benchmark results on standard bi-objective problems for small budget of evaluations are computed, which confirms that the new approach is more effective.

5.1 Background

Most optimization problems involve multiple objectives that need to be considered simultaneously and under certain constraints. Unlike single objective optimization, the result consists of multiple trade-off solutions called Pareto front. Over the last 20 years, Evolutionary Multi-objective Optimization (EMO) has demonstrated a great success in approximating the whole Pareto front. However, the ultimate goal of multi-objective optimization is to assist the decision maker to choose the most suitable solution in a preferred region. Therefore, the preference-based multi-objective optimization is a hot topic recently. It utilizes the preference information offered by the DM, such as weights, reference points, trade-off constraints, to guide the search towards the Region of Interest (ROI) on a Pareto front. The overview of existing approaches has already been provided in [82, 83, 84]. Depending on when the DM can participate in the optimization process, preference-based EMO can be categorized into three types: an *a-priori*, *a-posteriori*, *interactive*. In *a-priori* method, preference information from DM is provided before the search process, on the other hand in *a-posteriori* approaches; DM preferences are incorporated after the search. *Interactive* approaches make it possible to adapt the preference during optimization by having an interaction between the DM and EMO algorithms. The method proposed in this chapter belongs to the interactive methods.

According to the preference information offered by the DM, Bechikh et al. classified existing methods into weight-based approaches, solution ranking-based approaches, objective ranking-based approaches, reference point-based approaches, trade-off-based approaches, and outranking-based approaches [85]. There are also other methods to express preference, for example, utility function [86], lexicographic order [87], and preference region [88]. In the following, we restrict the summary of the state-of-art to approaches that use objective space region (or preferred region) as preference articulation.

Desirability Functions (DFs) is widely used to specify the preferences by transforming the objective values into a decision maker's satisfaction level, considering its simple and intuitive meaning. DFs can nonlinearly map the objectives in a desired region into the domain [0,1], based on the DFs' values of exemplary objective levels. Thus, an increasing desirability of the solution can reflect an increase of objective quality. By changing the values of objectives corresponding to 0 (least favored) and 1 (most favored), the DF can focus on different regions of the PF. It has already been successfully combined with NSGA-II [89], MOPSO [90], SMS-EMOA [91] on both benchmark problems and practical tuning problems from machining. Karahan and Köksalan devised a territory defining steady-state elitist evolutionary algorithm (TDEA) [92], which defines a territory around each solution to prevent crowding. They also proposed a preference-based approach, called prTDEA, to assign different sizes of territories for preferred regions and non-preferred regions. Preferred regions have smaller territories so that a denser coverage could be achieved. An interactive version of this method has been proposed in [93].

In [94], an interactive decision-making approach is embedded in the preference-inspired co-evolutionary algorithm (PICEA-g). The DM can easily brush his/her preferred region in the objective space without specifying any parameters. Goal vectors are generated according to this region and co-evolved with solution vectors, in order to achieve solutions in the ROI brushed by the DM. Other methods include weighted hypervolume [95] and hyperplane construction [96], all of which can be used to specify preferred regions.

Among the existing preference-based multiobjective optimization methods, surrogate-assisted optimization is rarely used. Moreover, the combination of TEHVI is meaningful and feasible when a DM has a vague idea about his/her preference region in the objective space, because TEHVI has an inherent ability to explore a certain region in the objective space. Specifying an interval region for each objective is also referred to as brushing or zooming, and it has already been applied in the context of interactive multicriteria optimization with non-expensive function evaluations by decision makers [94]. Here we introduce such techniques to surrogate assisted multiobjective optimization.

5.2 Algorithms

5.2.1 TEHVI-EGO for Preference-based Multi-Objective Optimization

For the aim of obtaining a preferred Pareto front, TEHVI-EGO is used in this chapter to solve this problem. The details of TEHVI calculation can be found in Chapter 4. Truncated domains $[\mathbf{A}, \mathbf{B}]$ are chosen according to a preferred region in objective space. The definition of preferred region is:

Definition 5.1 (Preferred region) *Given an objective space and two vectors, say* $\mathbf{A} \subset \mathbb{R}^2$ *and* $\mathbf{B} \subset \mathbb{R}^2$*, a preferred region (*PR*) is the area bounded by* $\mathbf{A}$ *and*

B *in the objective space:*

$$\mathrm{PR} = \left[\begin{pmatrix} A_1 \\ A_2 \end{pmatrix}, \begin{pmatrix} B_1 \\ B_2 \end{pmatrix} \right] \tag{2-1}$$

An example of preferred region is shown in Figure 5.1. The yellow region is a preferred region, and the boundary of this region is set for the truncated region for each objective function.

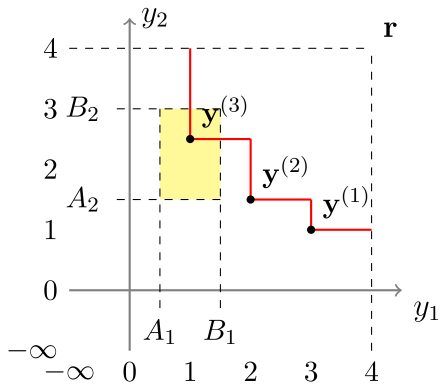

Figure 5.1: A preferred region for 2-D case.

The pseudocode for TEHVI-EGO with a preferred region is shown in Algorithm 6. It is important to compute a preliminary approximation of the Pareto front (line 3-6) before the preference region is set. This way the probability is increased and new non-dominated points can be found in this region. The interaction approach could be compared to 'zooming in' the preferred region or seen as a kind of brushing technique.

5.2.2 Preferred region with EAs

The concept of a preferred region can be integrated to the pre-selection criterion in Bayesian Global Optimization, and works well in Evolutionary Multi-objective Optimization. Our preferred region based Evolutionary Multi-Objective Algorithm model works reliably when the DM wants to concentrate only on those regions of the $\mathcal{P}$ which really interests him/her. For algorithms in this model, which include T-SMS-EMOA, T-R2-EMOA and T-NSGA-II (where T stands for preferred region), three ranking criteria (1. non-dominated sorting; 2. performance

Algorithm 6: TEHVI-EGO

Input: initialization size μ, termination criterion T_c, truncated boundary $[\mathbf{A}, \mathbf{B}]$, parameter ap

Output: Preferred Pareto front $\mathcal{PF}$

Initialize μ points and Pareto front $\mathcal{PF}$;
$g = 1$;
while $g <= ap$ **do**
    Set infill criterion as $EHVI$;
    Find the optimal point using CMA-ES;
    Update $\mathcal{PF}$ and $g = g + 1$;
DM interaction: Set $[\mathbf{A}, \mathbf{B}]$ as truncated boundary;
while $ap < g <= T_c$ **do**
    Set infill criterion as $TEHVI_{(\mathbf{A},\mathbf{B})}$;
    Find the optimal point by maximizing TEHVI (e.g., using CMA-ES);
    Update $\mathcal{PF}$ and $g = g + 1$;
Return $\mathcal{PF}$

indicator (Hypervolume in T-SMS-EMOA or R2 in T-R2-EMOA) or crowding distance in T-NSGA-II; 3. the Chebyshev distance to the preferred region) work together to achieve a well-converged and well-distributed set of Pareto optimal solutions in the preferred region using preference information provided by the DM. Non-dominated sorting is used as the first level ranking criterion, performance indicator or crowding distance as the second and the Chebyshev distance as the third level ranking criterion. The Chebyshev distance speeds up evolution toward the preferred region and is computed as the distance to the center of the preferred region.

The hypervolume, R2 indicator or crowding distance is chosen as the second level ranking criterion, which is used as a diversity mechanism and is measured based on coordinate transformations using desirability functions (DFs). The concept of desirability was introduced by Harrington [97] in the context of multi-objective industrial quality control and the approach of expressing the preferences of the DM using DFs is suggested by Wagner and Trautmann [91]. DFs map the objective values to desirabilities, which are normalized values in the interval [0,1], where the larger the value, the more satisfying the quality of the objective value. The Harrington DF [97] and Derringer-Suich DF [98] are two most common types of DFs and both of them result in biased distributions of the solutions on the $\mathcal{P}$ through mapping the objective values to desirabilities based on preference information. In our algorithm model, we use a simple type of DFs, which classifies the domain of the objective function into only two classes, "unacceptable" and "acceptable". In this approach we have:

$$D(x) = \begin{cases} 1 & x \text{ is in the preferred region,} \\ 0 & x \text{ is not in the preferred region.} \end{cases}$$

The desirability here is for a solution, it is not necessary to consider desirability by each objective because the goal of our algorithm is to *zoom in* the preferred region. Therefore, we treat solutions out of the preferred region as unacceptable solutions and assign their desirabilities to be 0; at the same time, we assume that all solutions inside the preferred region are of equal importance, (i.e. acceptable) and assign their desirabilities to be 1. There is no further bias on the points in the preferred region, however, if other types of DFs are integrated into the new algorithms, it is possible to generate solutions of different distributions in the preferred region concerning the specified preferences.

For solutions with desirability 0, their second level ranking criterion is assigned to be 0. For solutions with desirability 1, their second level ranking criterion needs to be calculated further. Because only solutions in the preferred region are retained, a way is derived to simplify the calculation of the indicator values or to realize a reference point free version of indicators [99], which is based on coordinate transformation. The preferred region is treated as a new coordinate space of which the origin being the lower bound. For the maximization problem in T-SMS-EMOA or the minimization problem in T-R2-EMOA, a coordinate transformation is performed for the i-th objective as:

$$Ct_i(x) = f_i(x) - LB(f_i)$$

For the minimization problems in T-SMS-EMOA or the maximization problems in T-R2-EMOA, coordinate transformation is performed for the i-th objective as:

$$Ct_i(x) = UB(f_i) - (f_i(x) - LB(f_i))$$

where $LB(f_i)$ and $UB(f_i)$ are the lower bound and upper bound of the i-th objective in the preferred region, which is predefined by the DM.

The reason for distinguishing the maximization from the minimization problems when performing coordinate transformation is that the origin of the new coordinate space (i.e., the lower bound of the target region) is used as the reference point when calculating the indicator values. In T-SMS-EMOA, the worst point in the target region is chosen as the reference point when calculating hypervolume. On the other hand, the ideal point is chosen as the reference point when calculating R2 indicator in T-R2-EMOA. After coordinate transformation, the calculation of the second-ranking criterion is implemented only in the target region instead of the whole coordinate system. It does make sense because the target region is the desired space to the DM. No reference point is needed in the calculation of crowding distance, and therefore, both formulas of coordinate transformation can be chosen in T-NSGA-II.

The shape of the target region is not necessarily rectangular; it could be a circle, an ellipse or any other shape, as long as the shape can sufficiently reflect whether a solution is in the target region or not. For instance, if the DM wants the solutions to be restricted to a sphere, he/she can specify the center point and radius of the sphere and our algorithms can obtain the approximation set of the $\mathcal{P}$ in the sphere.

T-SMS-EMOA The details of T-SMS-EMOA are given in Algorithm 7. The framework of T-SMS-EMOA is based on SMS-EMOA. However, after fast non-dominated sorting, all the solutions in the worst ranked front are seperated into two parts (acceptable and unacceptable) by the DF. Solutions in part 1 have desirability 0 and their hypervolume contributions are assigned to be 0; solutions in part 2 have desirability 1 and coordinate transformation is conducted on each objective of each solution in this part. After that, their hypervolume contributions are calculated in the new coordinate system and the origin in the new coordinate system is adopted as the reference point. The other difference between T-SMS-EMOA and SMS-EMOA is the involvement of the Chebyshev distance. In the early iterations, it is unlikely to exists individuals in the preferred region, the Chebyshev distance works on attracting solutions towards the preferred region.

T-R2-EMOA The details of T-R2-EMOA are given in Algorithm 8. R2-EMOA is extended to T-R2-EMOA in the same way as SMS-EMOA is extended to T-SMS-EMOA. The formula of coordinate transformation used in T-R2-EMOA, however, is opposite to the formula used in T-SMS-EMOA for the same problem, since the origin of the new coordinate system is used as the reference point in the measure of both hypervolume indicator in T-SMS-EMOA and R2 indicator in T-R2-EMOA.

Algorithm 7: T-SMS-EMOA

$P_0 \leftarrow$ init( ) /*Initialise random population*/
$t \leftarrow 0$
repeat
  $q_{t+1} \leftarrow$ generate(P_t) /*generate offspring by variation*/
  $P_t = P_t \cup \{q_{t+1}\}$
  $\{R_1, ..., R_v\} \leftarrow$ fast-nondominated-sorting(P_t)
  $\forall x \in R_v$: compute $D_{Ch}(x)$/* Chebyshev distance */
  $R_v = R_{v1} \cup R_{v2}$ /*separate acceptable and unacceptable parts:
  $\forall x \in R_{v1} : D(x) = 0; \forall x \in R_{v2} : D(x) = 1 * /$
  $\forall x \in R_{v1} : HC(x) = 0$
  $R_{v2} \leftarrow$ Coordinate Transformation(R_{v2})
  $\forall x \in R_{v2} : HC(x) = HV(R_{v2}) - HV(R_{v2} \backslash x)$
  if unique $argmin\{HC(x) : x \in R_v\}$ exists
    $x^* = argmin\{HC(x) : x \in R_v\}$
  else
    $x^* = argmax\{D_{Ch}(x) : x \in R_v\}$/*in case of tie, choose randomly*/
  $P_{t+1} = P \backslash \{x^*\}$
  $t \leftarrow t + 1$
until termination condition fulfilled

T-NSGA-II The details of T-NSGA-II are given in Algorithm 9. In T-NSGA-II, the size of the offsping population is the same as the size of the parent population. The next population is generated by choosing the best half solutions from the merged parent and offspring population: starting with points in the first non-domination front, continuing with points in the second non-domination front, and so on. Picking points in the descending order of crowding distance when all points in one non-domination front cannot be fully accommodated in P_{t+1} and picking points in the descending order of the Chebyshev distance when all the points with the same crowding distance can not be accommodated in P_{t+1}. Unlike T-SMS-EMOA and T-R2-EMOA, no reference point is needed in T-NSGA-II.

Algorithm 8: T-R2-EMOA

$P_0 \leftarrow$ init( ) /*Initialise random population*/
$t \leftarrow 0$
repeat
  $q_{t+1} \leftarrow$ generate(P_t) /*generate offspring by variation*/
  $P_t = P_t \cup \{q_{t+1}\}$
  $\{R_1, ..., R_v\} \leftarrow$ fast-nondominated-sorting(P_t)
  $\forall x \in R_v$: compute $D_{Ch}(x)$/* Chebyshev distance */
  $R_v = R_{v1} \cup R_{v2}$ /*separate acceptable and unacceptable parts:
  $\forall x \in R_{v1} : D(x) = 0; \forall x \in R_{v2} : D(x) = 1 * /$
  $\forall x \in R_{v1} : r(x) = 0$
  $R_{v2} \leftarrow$ Coordinate Transformation(R_{v2})
  $\forall x \in R_{v2} : r(x) = R2(P \backslash \{x\}; \Lambda; i) / * i$: ideal point*/
  if unique $argmin\{r(x) : x \in R_v\}$ exists
    $x^* = argmin\{r(x) : x \in R_v\}$
  else
    $x^* = argmax\{D_{Ch}(x) : x \in R_v\}$/*in case of tie, choose randomly*/
  $P_{t+1} = P \backslash \{x^*\}$
  $t \leftarrow t + 1$
until termination condition fulfilled

5.3 Empirical Experiments

5.3.1 TEHVI assisted EGO

Experimental Setup All the experiments were based on the same computer and the hardware were: Intel(R) i7-3770 CPU @ 3.40GHz, RAM 16GB. The operating system was Ubuntu 14.04 LTS (64 bit), and software were gcc 4.9.2 with compiler flag -Ofast for exact TEHVI calculation, and MATLAB 8.4.0.150421 (R2014b), 64 bit for EGO. The benchmarks were: ZDT1, ZDT2 and the generalized Schaffer problem (GSP) [81], with the parameter of $\gamma = 0.4$. Each experiment was repeated once. The preference regions were set as in Table 5.1: The number of initial points for all the experiments was set to 30, and the iteration number was set to 300. After initialization, 30 iterations based on TEHVI with prefer-

Algorithm 9: T-NSGA-II

```
P_0 ← init( ) /*Initialise random population*/
t ← 0
repeat
   Q_t ← generate(P_t) /*generate offsprings by variation*/
   P_t = P_t ∪ Q_t
   ∀x ∈ P_t : compute D_Ch(x)/* Chebyshev distance */
   {R_1, ..., R_v} ← fast-nondominated-sorting(P_t)
   for i = rank 1,...,v do
      R_i = R_i1 ∪ R_i2 /*separate acceptable and unacceptable parts*/
      ∀x ∈ R_i1 : D_c(x) = 0/ * D_c: crowding distance*/
      R_i2 ← Coordinate Transformation(R_i2)
      ∀x ∈ R_i2 : compute D_c(x)
   P_{t+1} ← half of P_t based on rank, D_c and then D_Ch
   t ← t + 1
until termination condition fulfilled
```

Table 5.1: Parameter settings.

Benchmark	rg. 1		rg. 2		rg. 3		rg. 4	
	$[A_1, B_1]$	$[A_2, B_2]$	$[A_1, B_1]$	$[A_2, B_2]$	$[A_1, B_1]$	$[A_2, B_2]$	$[A_1, B_1]$	$[A_2, B_2]$
GSP	$[0, \infty]$	$[0, \infty]$	$[0, 0.1]$	$[0.5, 1]$	$[0, 0.5]$	$[0, 0.5]$	$[0.5, 1]$	$[0, 0.1]$
ZDT1	$[0, \infty]$	$[0, \infty]$	$[0, 0.5]$	$[0.5, 1]$	$[0, 0.5]$	$[0, 0.5]$	$[0.5, 1]$	$[0, 0.5]$
ZDT2	$[0, \infty]$	$[0, \infty]$	$[0, 0.5]$	$[0.5, 1]$	$[0, 0.5]$	$[0, 0.5]$	$[0.5, 1]$	$[0, 0.5]$

ence region of $\mathbf{A} = (0,0)^T$ and $\mathbf{B} = (\infty,\infty)^T$ were performed for obtaining a preliminary Pareto front approximation. Then the rest of 240 iterations results, which based on the truncated domain with the precise preferred regions, is shown in Table 5.2.

Empirical Results The experimental results for GSP, ZDT1 and ZDT2 problems are shown in Figure 5.2, 5.3 and 5.4 respectively. Each upper left subfigure is a Pareto front without preferred region (or, a preferred region is set as $(\mathbf{A}, \mathbf{B}) = (\mathbf{0}^T, \boldsymbol{\infty}^T)$. The yellow region in each figure ((b),(c) and(d)) represents the preference region.

The experiments show that most elements in a Pareto front concentrate on the

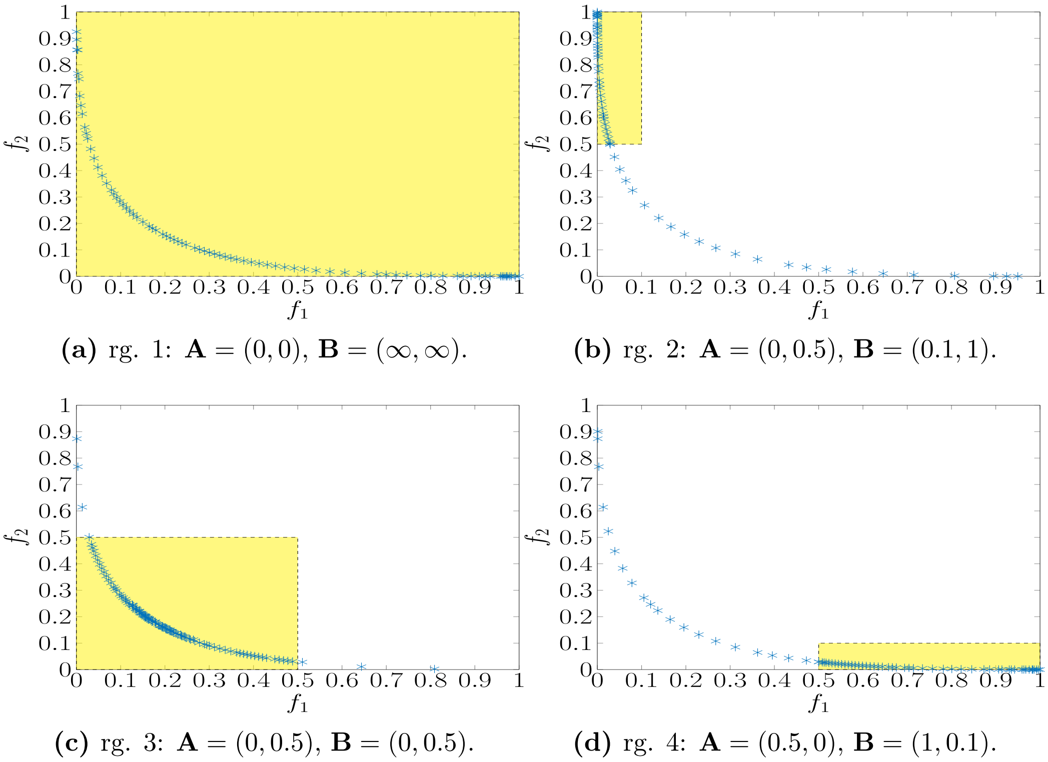

(a) rg. 1: $\mathbf{A} = (0, 0)$, $\mathbf{B} = (\infty, \infty)$.

(b) rg. 2: $\mathbf{A} = (0, 0.5)$, $\mathbf{B} = (0.1, 1)$.

(c) rg. 3: $\mathbf{A} = (0, 0.5)$, $\mathbf{B} = (0, 0.5)$.

(d) rg. 4: $\mathbf{A} = (0.5, 0)$, $\mathbf{B} = (1, 0.1)$.

Figure 5.2: The preferred Pareto front for GSP problem.

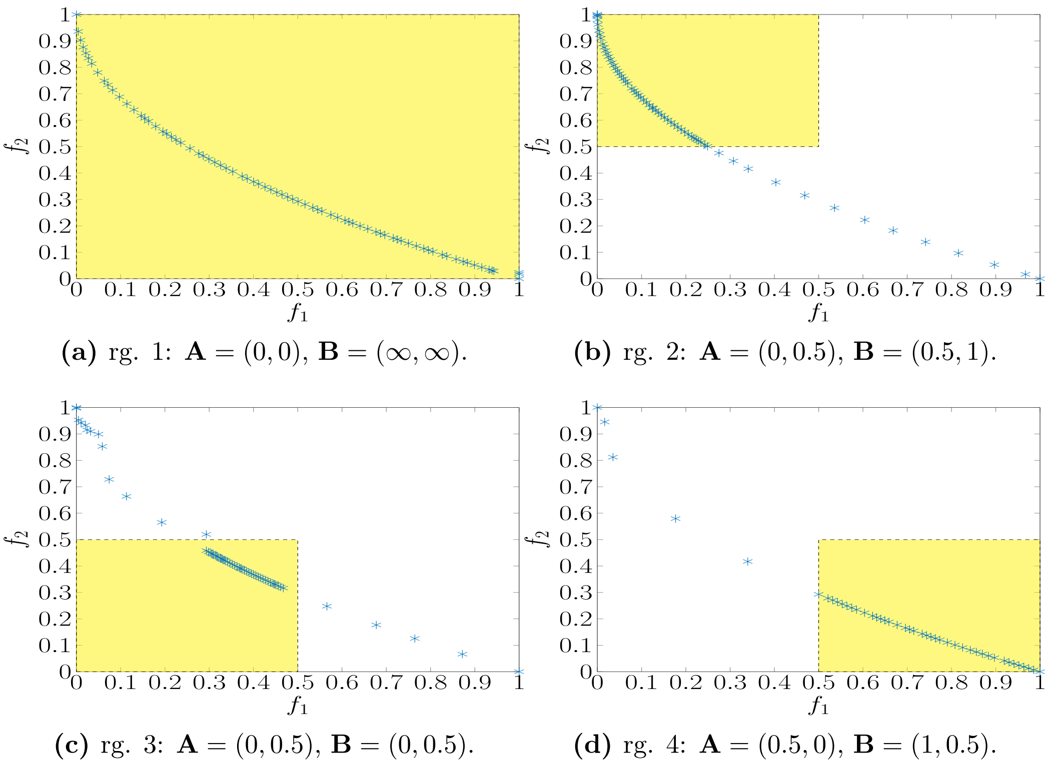

(a) rg. 1: $\mathbf{A} = (0, 0)$, $\mathbf{B} = (\infty, \infty)$.

(b) rg. 2: $\mathbf{A} = (0, 0.5)$, $\mathbf{B} = (0.5, 1)$.

(c) rg. 3: $\mathbf{A} = (0, 0.5)$, $\mathbf{B} = (0, 0.5)$.

(d) rg. 4: $\mathbf{A} = (0.5, 0)$, $\mathbf{B} = (1, 0.5)$.

Figure 5.3: The preferred Pareto front for ZDT1 problem.

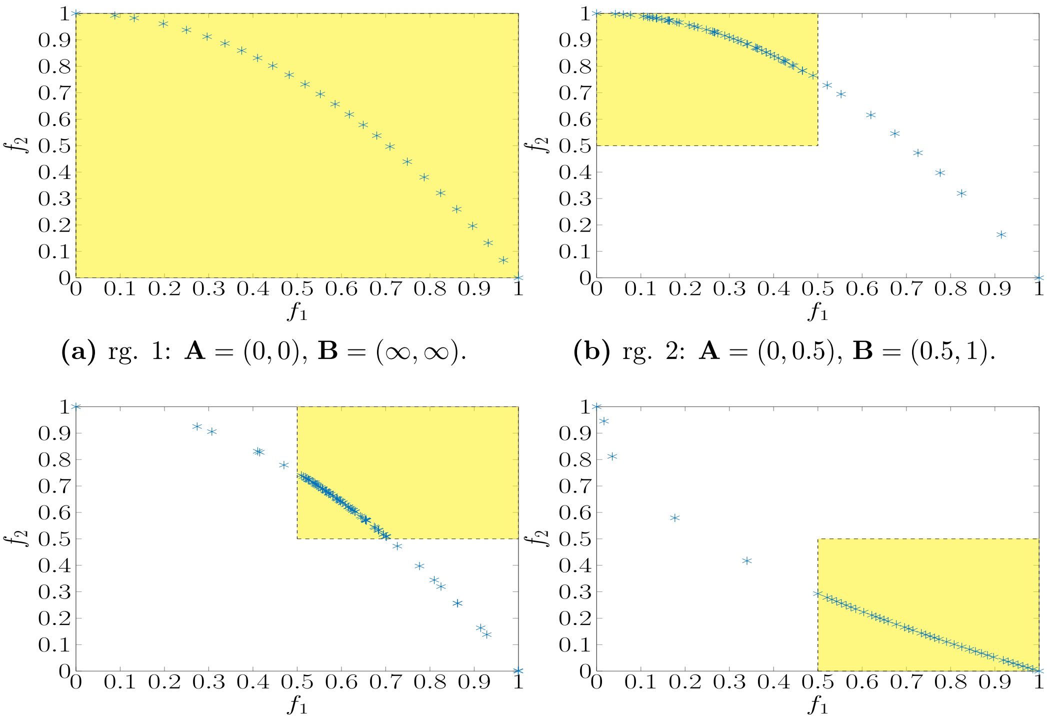

(a) rg. 1: $\mathbf{A} = (0, 0)$, $\mathbf{B} = (\infty, \infty)$.

(b) rg. 2: $\mathbf{A} = (0, 0.5)$, $\mathbf{B} = (0.5, 1)$.

(c) rg. 3: $\mathbf{A} = (0, 0.5)$, $\mathbf{B} = (0, 0.5)$.

(d) rg. 4: $\mathbf{A} = (0.5, 0)$, $\mathbf{B} = (1, 0.5)$.

Figure 5.4: The preferred Pareto front for ZDT2 problem.

Table 5.2: The size of Pareto front analysis.

Benchmark	n			
	rg. 1	rg. 2	rg. 3	rg. 4
GSP	112	64	115	70
ZDT1	77	78	58	80
ZDT2	112	64	115	70

corresponding preferred region, and they are adjacent to the true Pareto front. Moreover, the Pareto front approximation in a preferred region also covers the extreme boundary in this area. Since the truncated probability density function is not zero only in the truncated domain, TEHVI is not zero only in a preferred region and zero outside of the preferred region. Because of this, EGO can intensively explore the preferred region in the objective space. Some solutions exist in the outside preferred region. This is reasonable, considering the initialization and only 30 precise evaluations. Moreover, all these procedures are explorations in the whole objective space. In the case of ZDT1 problem, the Pareto front with the preferred region in Figure 5.3 (b) can not explore the extreme boundary in the preferred region. This is probably caused by a failure of the CMA-ES [100] to locate points in this narrow part. It might be advisable to widen the interval range in such cases.

5.3.2 Preferred region based on EAs[1]

Experimental Settings In this section, simulations are conducted to demonstrate the performance of the algorithms, namely T-SMS-EMOA, T-R2-EMOA, and T-NSGA-II. In all simulations, we use the SBX operator with an index of 15 and polynomial mutation with an index 20 [101]. The crossover and mutation probabilities are set to 1 and $1/N$, respectively.

We conduct experiments on some benchmark problems, including ZDT, DTLZ and knapsack problems, to investigate the performance of the new algorithms. All experiments were run on a personal laptop with i5-5257U @ 2.7 GHz and 8G RAM. The population size and the number of evaluations are chosen to be dependent on the complexity of the test problem. Table 5.3 shows the population size and the number of evaluations (NOEs) we use on different test problems.

Table 5.3: Population Size and Number of Evaluations.

Problems	Population Size	NOEs
ZDT1	100	10000
ZDT2-3	100	20000
DTLZ1-2	100	30000
knapsack-250-2 knapsack-500-2	200	200000
knapsack-250-3 knapsack-500-3	250	500000

Experimental Results

Two-Objective ZDT Test Problems In this section, we consider three ZDT test problems. First, we consider the 30-variable ZDT1 problem. This problem

[1]This part of work is mainly done by Yali Wang.

has a convex Pareto optimal front which is a connected curve and can be determined by $f_2(x) = 1 - \sqrt{f_1(x)}$. The true $\mathcal{P}$ spans continuously in $f_1 \in [0, 1]$. Four different preferred regions are chosen to observe the performance of T-SMS-EMOA, T-R2-EMOA and T-NSGA-II in Figure 5.5, Figure 5.6 (a) and Figure 5.6 (b), respectively. The first preferred region covers the entire $\mathcal{P}$ with the lower bound (0,0) and the upper bound (1,1). The second preferred region restricts preferred solutions to the central part of the $\mathcal{P}$ and its lower bound is (0.1,0.1), and upper bound is (0.5,0.5). The third and fourth preferred regions take two ends of the $\mathcal{P}$, respectively and have their lower bounds to be (0,0.6) and (0.6,0), upper bounds to be (0.3,1) and (1,0.3), respectively.

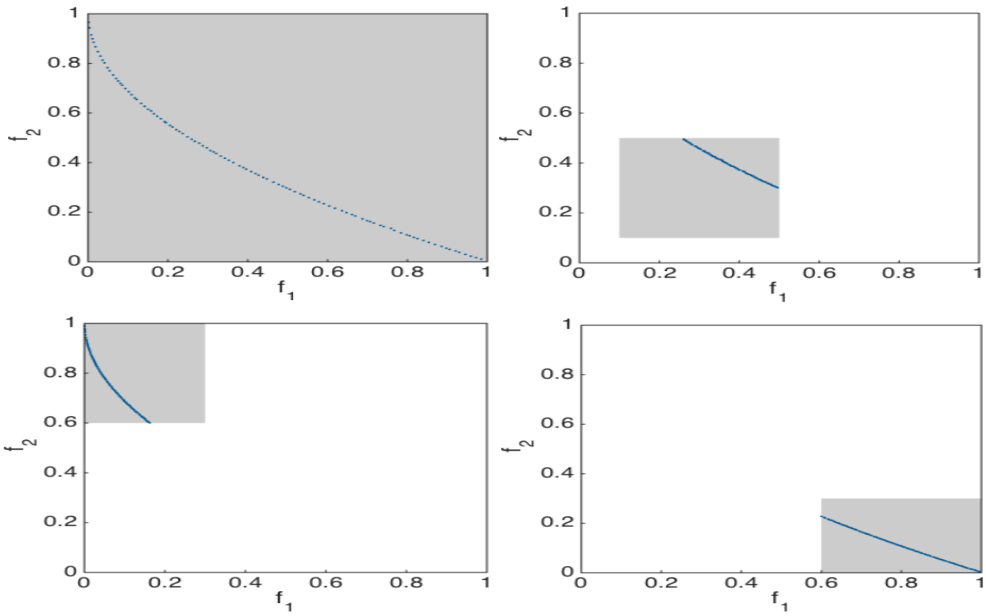

Figure 5.5: Representative $\mathcal{P}$ approximations of T-SMS-EMOA on ZDT1. The different preferred regions are highlighted by gray boxes and their lower and upper bounds are: upper left graph: (0,0)(1,1), upper right graph: (0.1,0.1)(0.5,0.5), lower left graph: (0,0.6)(0.3,1), lower right graph: (0.6,0)(1,0.3).

Figure 5.5 and Figure 5.6 ((a) and (b)) show $\mathcal{P}$ approximations obtained from the algorithms on the four different preferred regions in a random single run. It is observed that all three algorithms can find well-distributed and well-converged solutions on the $\mathcal{P}$ in the preferred regions and no outliers exist. The solution set obtained by T-SMS-EMOA is more uniform than the solution sets obtained by the other two algorithms. It is also observable that R2 indicator has a bias towards the center of the PF.

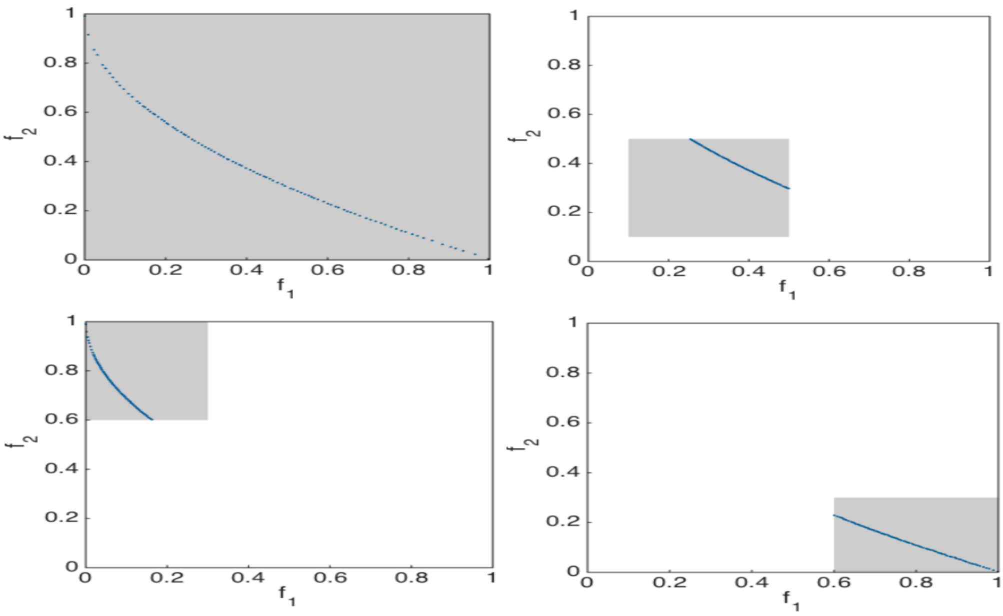

(a) Representative $\mathcal{P}$ approximations of T-R2-EMOA on ZDT1. The different preferred regions are highlighted by gray boxes and their lower and upper bounds are: upper left graph: (0,0)(1,1), upper right graph: (0.1,0.1)(0.5,0.5), lower left graph: (0,0.6)(0.3,1), lower right graph: (0.6,0)(1,0.3).

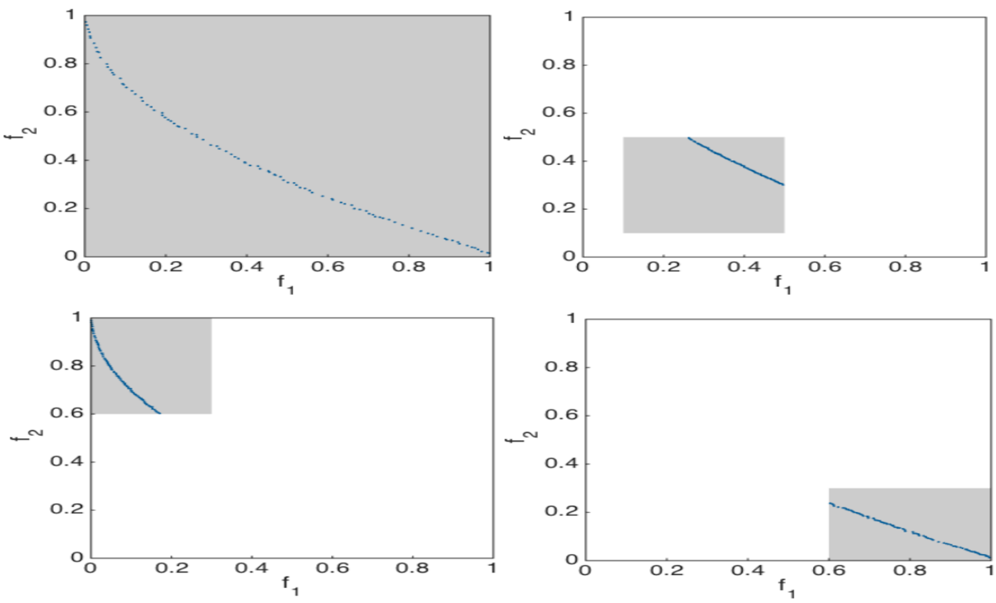

(b) Representative $\mathcal{P}$ approximations of T-NSGA-II on ZDT1. The different preferred regions are highlighted by gray boxes and their lower and upper bounds are: upper left graph: (0,0)(1,1), upper right graph: (0.1,0.1)(0.5,0.5), lower left graph: (0,0.6)(0.3,1), lower right graph: (0.6,0)(1,0.3).

Figure 5.6: The preferred Pareto fronts for ZDT1 problem.

We examine the performance of new algorithms using the hypervolume metric. The hypervolume is calculated within the preferred region by normalizing the values of each objective to the values between 0 and 1 and using the lower bound of the preferred region as the reference point for the maximization problem and the upper bound of a preferred region as the reference point for the minimization problem. Table 5.4 shows the median of hypervolume over 30 runs. The statistical results correspond to the observation that T-SMS-EMOA outperforms T-R2-EMOA and T-NSGA-II slightly. The original SMS-EMOA, R2-EMOA and NSGA-II are also involved in the comparison, and the results of the original MOEAs are obtained by presenting constraints in the description of a problem. Although the results of our algorithms are not better than those of original MOEAs with constraints on the range of objectives, experiments show that our algorithms can reduce computation time dramatically.

Table 5.4: The median of hypervolume and average computation time (Sec.) on ZDT1 with respect to different preferred regions.

New Algorithms		T-SMS-EMOA	T-R2-EMOA	T-NSGA-II
preferred region	Metric			
(0,0)	HV	0.6580	0.6566	0.6425
(1,1)	Time	24.99	74.01	0.21
(0.1,0.1)	HV	0.1640*	0.1638*	0.1543
(0.5,0.5)	Time	10.30	23.61	0.19
(0,0.6)	HV	0.8110	0.8097	0.7936
(0.3,1)	Time	12.86	31.78	0.20
(0.6,0)	HV	0.6255*	0.6233*	0.6079
(1,0.3)	Time	11.45	27.92	0.21
Original Algorithms		SMS-EMOA	R2-EMOA	NSGA-II
(0,0)	HV	0.6621	0.6610	0.6609
(1,1)	Time	108.57	314.99	0.25
(0.1,0.1)	HV	0.1694	0.1693	0.1690
(0.5,0.5)	Time	106.32	274.05	0.23
(0,0.6)	HV	0.8197	0.8185	0.8191
(0.3,1)	Time	105.73	271.00	0.21
(0.6,0)	HV	0.6364	0.6348	0.6356
(1,0.3)	Time	101.82	283.3	0.22

In the table, the symbol of "$*$" on the values for the same preferred region means the medians of these algorithms are significantly indifferent. The Mann-Whitney U test (also called the Mann-Whitney-Wilcoxon (MWW), Wilcoxon rank-sum test, or Wilcoxon-Mann-Whitney test) is used to determine whether the medians of different algorithms for the same problem are significantly indifferent.

Next, we consider the 30-variable ZDT2 and ZDT3 problems. ZDT2 has a non-convex Pareto optimal front, and ZDT3 has a disconnected Pareto optimal front, which consists of five non-contiguous convex parts. Circle preferred regions are adopted in the case of ZDT2 and ZDT3 problems. A circle with a center point (1,0) and radius 0.5 intersects the whole $\mathcal{P}$ of ZDT2 at its one end, and a circle with a center point (0.6,0.5) and radius 0.3 intersects the whole $\mathcal{P}$ at its central part. The two different circles are chosen as examples for preferred regions on the ZDT2 problem. Experiments for a circle with a center point (0.3,0.1) and radius 0.3 as the preferred region are conducted on the ZDT3 problem.

Figure 5.7 shows PF approximation of T-SMS-EMOA in these preferred regions. Similar figures can also be achieved by T-R2-EMOA and T-NSGA-II. Orange points denote the results obtained by means of T-SMS-EMOA on provided preference information. Approximated optimal $\mathcal{P}$ of ZDT2 problem for 100 blue points are from [102]. Statistical results of the median of hypervolume for three algorithms (T-SMS-EMOA, T-R2-EMOA and T-NSGA-II) for 30 independent runs in each preferred region are shown in Table 5.5.

Table 5.5: The median of hypervolume on ZDT2 and ZDT3 with respect to different circle preferred regions.

MOEA / preferred region	T-SMS-EMOA	T-R2-EMOA	T-NSGA-II
ZDT2 (1,0) 0.5	0.3168	0.3167	0.3159
ZDT2 (0.6,0.5) 0.3	0.3257	0.3256	0.3234
ZDT3 (0.3,0.1) 0.3	0.3377	0.3375	0.3365

5.4 Summary

This chapter introduced two main approaches to solve the preference-based multi-objective optimization problems. The first approach is using TEHVI as the pre-selection criterion in MOBGO. The basic idea behind TEHVI-EGO is straightfor-

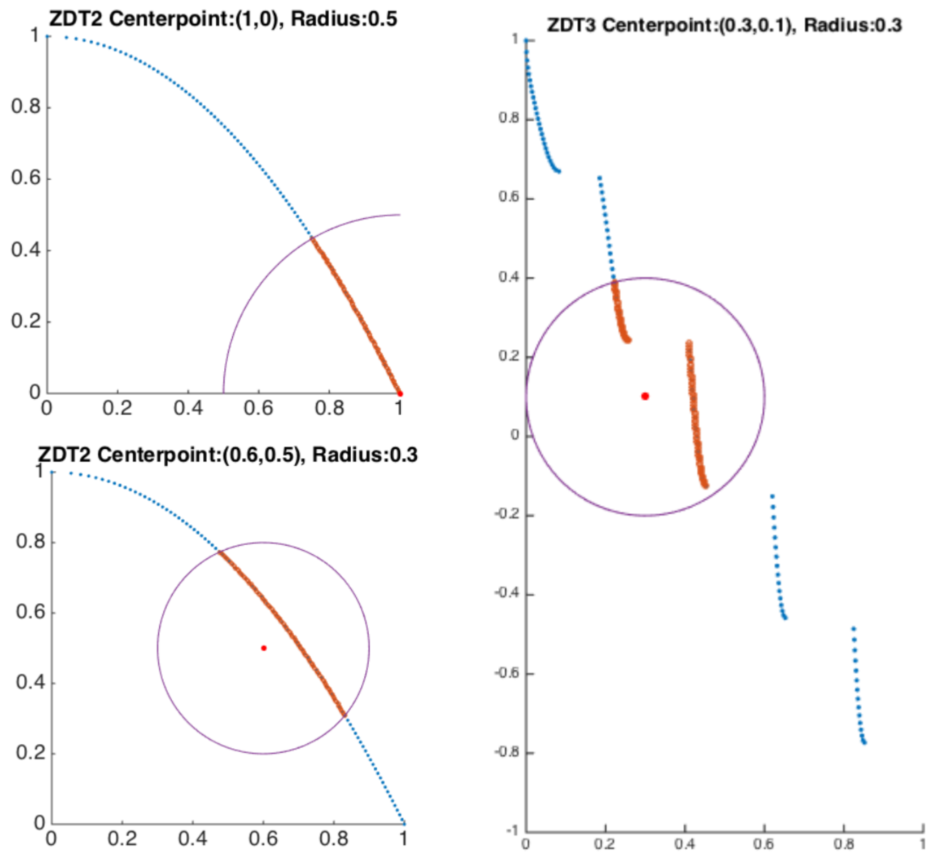

Figure 5.7: Representative $\mathcal{P}$ approximations of T-SMS-EMOA on ZDT2 and ZDT3. The preferred regions are purple circles and center points are red points.

ward: using the lower and upper bounds in THEIV to define the preferred region in the objective space, TEHVI can lead the algorithm to explore more solutions in this preferred region. TEHVI-EGO for solving the problem of preference-based multiobjective optimization is introduced. The concept of a preferred region is introduced by means of the corresponding truncated domain in TEHVI (interval range in objective space). Then, EGO can intensively explore the preferred region in objective space, and obtain preferred parts of the Pareto front. Empirical experiments were based on GSP, ZDT1 and ZDT2 problems, and show that a Pareto front can effectively converge to a preferred region through the proposed method. Compared to non-preference method, the population of the points in a preference region is larger, which means more choices are provided in this preference region. The computational cost remains small – $O(n \log n)$ for a current

Pareto front consisting of n points. In summary, TEHVI-EGO shows a robust capability to search Pareto front segments in a particularly preferred region.

Inspired by the definition of TEHVI, preferred region based EAs are proposed and introduced in the second approach. In this chapter, a region-based multi-objective evolutionary algorithm model is also proposed. Three algorithms named T-SMS-EMOA, T-R2-EMOA and T-NSGA-II have been instantiated when combining the algorithm model with original SMS-EMOA, R2-EMOA and NSGA-II algorithms. These new algorithms have been applied to some continuous benchmark problems with two objectives. Experimental results show that our algorithms can guide the search toward the preferred region on the Pareto optimal front. No outlier appears on a reasonable number of function evaluations. Although our new algorithms presented similar performance with the original MOEAs on tested problems by integrating accessorial constraints in the problem description, our algorithms save computational efforts by guiding the search towards the preferred region without exploring the whole set of Pareto optimal solutions. On the contrary, in the case of original MOEAs, the increase in the number of constraints leads to the decrease of the search ability. Moreover, the proposed algorithms exhibit the trend of behaving better with the increase in the number of objectives, compared to the original MOEAs. The experiments on many-objective problems (i.e., problems with four or more objectives) should be conducted in future work.